

TIME-REVERSAL SPACE-TIME CODES IN ASYNCHRONOUS TWO-WAY DOUBLE-ANTENNA RELAY NETWORKS

Yun Liu^{*}, Wei Zhang[†], and P. C. Ching^{*}

^{*} Department of Electronic Engineering, The Chinese University of Hong Kong, Hong Kong, China

[†] School of Electrical Engineering & Telecommunications, The University of New South Wales, Australia

Emails: yliu@ee.cuhk.edu.hk; wzhang@ee.unsw.edu.au; pcching@ee.cuhk.edu.hk

ABSTRACT

We consider an asynchronous two-way relay network, in which two double-antenna relays assist in the communication between two single-antenna terminals through analog network coding. The asynchronous transmission between relays and terminals causes symbol misalignments and results in diversity loss in space-time block code (STBC). We propose a zero-padded time-reversal quasi-orthogonal STBC that can achieve full diversity with low-complexity maximum likelihood (ML) decoding, given a bounded delay. With ML decoding, the proposed code is decomposed into several independent parts, which leads to single complex symbol decoding. Proof of full diversity is established, and the decoding complexity order is analyzed for the proposed design. Simulations confirm the full diversity gain. The bit error rate performance in asynchronous scenarios is almost the same as that in synchronous scenarios.

Index Terms— Asynchronous, two-way relay network, analog network coding, space-time code, full diversity, maximum likelihood decoding.

1. INTRODUCTION

Two-way relay networks allow simultaneous information exchange between two terminals via a few relays in between [1–4]. In Phase I, both terminals simultaneously broadcast their signals to relays. Depending on how signal mixing on relays, individual relay could choose to either map the mixed signals to the network-coded symbols, which is known as digital network coding [5–7], or directly amplify and transmit the received superposition signals, which is called analog network coding (ANC) [8]. In Phase II, the relays simultaneously broadcast to terminals. Terminals extract useful signals by cancelling self-interference components. The channel between multiple relays and each terminal is a multiple-input single-output (MISO) channel, which offers diversity gain. Space-time block code (STBC) [9–12] can harvest the diversity gain in such MISO channel.

Given different path and processing delays on each relay, multiple transmission undertaken by distributed nodes may not be perfectly synchronized over time. In two-way relay networks, such asynchronous transmission is received by relays in Phase I and terminals in Phase II. The lack of perfect synchronization may cause severe performance degradation, such as diversity loss in STBC [13, 14]. To compensate for the asynchronous transmission, synchronization procedures are required. However, such procedures normally require considerable overhead. To avoid unnecessary overhead, asynchronous STBC [14–26] is proposed to achieve diversity gain without synchronization requirement. For one-way relay networks, some STBC designs have been used to achieve diversity gain.

However, one-way relay networks do not have asynchronous transmission on relays, and the existence of such asynchronous transmission render these studies inapplicable to two-way relay networks.

Recently, several schemes have reconsidered the asynchronous issue in two-way relay networks [27–30]. These schemes can be categorized as either frequency-domain or time-domain approaches. For frequency-domain approaches, the authors in [28, 29] considered frequency selective fading channel and adopted orthogonal frequency division multiplexing (OFDM), in which cyclic prefix was applied to combat symbol misalignment. Thus, such approaches may not be applicable to non-OFDM systems. A time-domain approach was proposed in [27] to achieve full diversity through distributed linear convolutive STBC [20]. However, maximum likelihood (ML) decoding of this time-domain approach is computationally prohibitive. First, the ML decoding in this approach requires an exhaustive search over all symbols. Second, for different delay differences, the received signal structures also differ, and thus result in different ML decoders. Consequently, the complexity of ML decoding increases exponentially with code length and linearly with the maximum delay difference. To alleviate ML decoding complexity, zero-padded interleave-reversal Alamouti code (ZP-IR AC) [30] has been proposed to achieve diversity order 2 with reduced ML decoding complexity. However, ZP-IR AC is limited to networks with two single-antenna relays, and can only provide transmit diversity order 2. Moreover, the ML decoding complexity of ZP-IR AC continues to increase with the constellation size to the fourth power, which may be a problem for high-order constellations. This drawback motivates us to design a new type of STBC to achieve full diversity order higher than 2 with simpler complexity order than ZP-IR AC for ANC and multiple antennas at relays.

Time-reversal STBC (TR-STBC) [14] has been proposed in one-way cooperative communication with two single-antenna transmitters and one destination. However, owing to the existence of asynchronous transmission received by relays, TR-STBC can not be directly applied to asynchronous two-way relay networks. For 4×1 systems, quasi-orthogonal space-time block code (QOSTBC) [31] successfully achieves full rate 1 and full diversity order 4 with single symbol complexity. Our following work on two double-antenna relays is based on QOSTBC.

In this paper, we propose a zero-padded time-reversal quasi-orthogonal space-time block code (ZP-TR QOSTBC) for asynchronous two-way relay networks with two double-antenna relays. Given the maximum delay difference, terminals transmit with zero padding to combat asynchronous transmission received by relays in Phase I. One relay then processes a time-reversal procedure on the received signals and broadcast the signals at Phase II with the other relay. After cancelling self-interference, the overall decod-

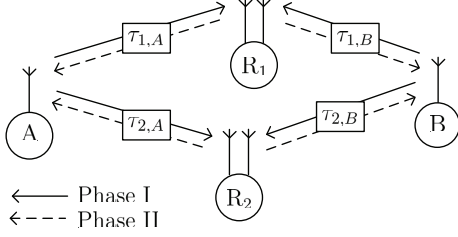


Fig. 1: Asynchronous two-way relay network with two relay nodes.

ing problem is decomposed into several independent sub-problems, which greatly facilitate the ML decoding process. The proposed code achieve full diversity order 4 with ML decoding complexity of $\mathcal{O}(L|S|)$, where L is the code length and $|S|$ is the cardinality of the signal constellation. Proof of full diversity, code rate analysis and decoding complexity analysis are provided for the proposed codes.

The remainder of this paper is organized as follows. Section 2 provides the system model of asynchronous two-way relay networks. The proposed STBC code design is presented in Section 3. Section 4 provides the simulation results, and Section 5 presents the conclusion.

Notation: Vector $\mathbf{x}[i:j]$ represents a sub-vector in \mathbf{x} from index i to index j . We allow $j < i$. If $i < j$, then $\mathbf{x}[i:j] = [x[i], x[i+1], \dots, x[j]]$; if $i > j$, then $\mathbf{x}[i:j] = [x[i], x[i-1], \dots, x[j]]$. $x^*[i]$ represents the conjugate signal of $x[i]$.

2. SYSTEM MODEL

A two-way relay network consists of two double-antenna relay nodes R_1, R_2 , assisting in the information exchange between single-antenna terminals A and B , as shown in Fig. 1. Each node operates in half-duplex mode, which means nodes could not transmit and receive at the same time. The cooperation between relays is exploited to provide diversity gain in data transmission. In Phase I, the channel fading coefficient from terminal J to R_i is $\mathbf{h}_{i,J}$; in Phase II, the channel fading coefficient from R_i to terminal J is $\hat{\mathbf{h}}_{i,J}$, where $i = 1, 2$ and $J = A, B$. The channel fading coefficient is known at the receiver side. The path delay between R_i and terminal J is $\tau_{i,J}$, where $i = 1, 2$ and $J = A, B$. The delay difference bound is denoted by T , where $|\tau_{i,J} - \tau_{i,j}| \leq T$, $[i, J] \neq [\hat{i}, \hat{J}]$, $i, \hat{i} \in \{1, 2, \dots, N\}$ and $J, \hat{J} \in \{A, B\}$. $\tau_{i,J}$ is an integer multiple of symbol duration. The fractional part of $\tau_{i,J}$ can be regarded as multipath effects addressed by equalizers through oversampling [17].

The network employs ANC. In Phase I, the relays receive the signal vector of sequence \mathbf{a} from terminal A and the signal vector of sequence \mathbf{b} from terminal B . The relays then perform some transformation on the received signals to obtain new signal vectors. In Phase II, the relays amplify and forward their new signal vectors to terminals A and B simultaneously. α_i is the amplifying factor at R_i to ensure same power on both relays, where $i = 1, 2$.

3. ZERO-PADDED TIME-REVERSAL SPACE-TIME CODES

ZP-IR AC [30] achieves diversity order 2 with complexity $\mathcal{O}(L|S|^4)$. By using a different code construction method, we pro-

pose ZP-TR QOSTBC to achieve higher diversity order and lower complexity order than that of ZP-IR AC for a network with two double-antenna relays.

3.1. Code Structure

Terminal A transmits sequence \mathbf{a} of 4ℓ symbols, and terminal B transmits sequence \mathbf{b} of 4ℓ symbols, where $\ell \in \mathbb{Z}_+$. Both \mathbf{a} and \mathbf{b} adopt stretched constellations [31], such as $c_1 + k_1 c_2$, where $c_1, c_2 \in \mathbb{Z}$, and k_1 is an irrational number like $\sqrt{2}$.

• In Phase I, terminals form groups of ℓ symbols each, and insert an all-zero row vector with T elements, $\mathbf{0}_T$, between each group, to construct $\hat{\mathbf{a}}$ and $\hat{\mathbf{b}}$ as follows:

$$\hat{\mathbf{a}} = [\mathbf{a}[1 : \ell], \mathbf{0}_T, \mathbf{a}[\ell+1 : 2\ell], \mathbf{0}_T, \mathbf{a}[2\ell+1 : 3\ell], \mathbf{0}_T, \mathbf{a}[3\ell+1 : 4\ell]]$$

$$\hat{\mathbf{b}} = [\mathbf{b}[1 : \ell], \mathbf{0}_T, \mathbf{b}[\ell+1 : 2\ell], \mathbf{0}_T, \mathbf{b}[2\ell+1 : 3\ell], \mathbf{0}_T, \mathbf{b}[3\ell+1 : 4\ell]].$$

Zero-padding is employed to accommodate symbol misalignment at the relays. The signal matrix received by the two antennas on R_i is

$$\mathbf{Y}_{R_i} = \sqrt{P_T} [\mathbf{h}_{i,A}, \mathbf{h}_{i,B}] \begin{bmatrix} \mathbf{0}_{\tau_{i,A}} & \hat{\mathbf{a}} & \mathbf{0}_{[\Delta_i]^+} \\ \mathbf{0}_{\tau_{i,B}} & \hat{\mathbf{b}} & \mathbf{0}_{[-\Delta_i]^+} \end{bmatrix} + \mathbf{N}_{R_i}$$

where $\mathbf{h}_{i,A} = [h_{i,A,1}, h_{i,A,2}]^T$, $\mathbf{h}_{i,B} = [h_{i,B,1}, h_{i,B,2}]^T$, $\Delta_i \triangleq \tau_{i,B} - \tau_{i,A}$, and $i = 1, 2$.

Given that the two antennas of R_i receive two copies of the same transmitted signal, R_i obtains the results of the combination as

$$\mathbf{y}_{R_i} = \mathbf{k}_i \mathbf{Y}_{R_i}$$

where \mathbf{k}_i is the signal combining row vector of length 2. As will be seen later, \mathbf{k}_i can be any nonzero vector without losing the full diversity.

\mathbf{y}_{R_i} is separated into four parts as

$$\mathbf{y}_{R_i,j}[1 : \ell + |\Delta_i|]$$

$$= \mathbf{y}_{R_i} \left[\min\{\tau_{i,A}, \tau_{i,B}\} + (j-1)\ell + (j-1)T + 1 : \right.$$

$$\left. \max\{\tau_{i,A}, \tau_{i,B}\} + j\ell + (j-1)T \right],$$

where $i = 1, 2$, and $j = 1, 2, 3, 4$.

The relays will organize the four parts of the signals following QOSTBC structure as follows.

$$\begin{bmatrix} \mathbf{y}_{R_1,1} & \mathbf{y}_{R_1,2} & \mathbf{y}_{R_1,3} & \mathbf{y}_{R_1,4} \\ -\mathbf{y}_{R_1,2}^* & \mathbf{y}_{R_1,1}^* & \mathbf{y}_{R_1,4}^* & -\mathbf{y}_{R_1,3}^* \\ -\mathbf{y}_{R_2,3}^* & -\mathbf{y}_{R_2,4}^* & \mathbf{y}_{R_2,1}^* & \mathbf{y}_{R_2,2}^* \\ -\mathbf{y}_{R_2,4}^* & \mathbf{y}_{R_2,3}^* & -\mathbf{y}_{R_2,2}^* & \mathbf{y}_{R_2,1}^* \end{bmatrix}. \quad (1)$$

To address the symbol misalignment issue, some zero padding blocks are added at relays. Details of the signals design at relays are given below.

R_1 constructs $\hat{\mathbf{y}}_{R_1,1}$ and $\hat{\mathbf{y}}_{R_1,2}$ by inserting all-zero row vectors, each with $2T - |\Delta_1|$ elements, between $\mathbf{y}_{R_1,j}$ as follows:

$$\hat{\mathbf{y}}_{R_1,1} = \alpha_1 [\mathbf{y}_{R_1,1}, \mathbf{0}_{2T-|\Delta_1|}, \mathbf{y}_{R_1,2}, \mathbf{0}_{2T-|\Delta_1|}, \mathbf{y}_{R_1,3}, \mathbf{0}_{2T-|\Delta_1|}, \mathbf{y}_{R_1,4}]$$

$$= \hat{\mathbf{n}}_{R_1,1} + \alpha_1 \sqrt{P_T} [\mathbf{k}_1 \mathbf{h}_{1,A}, \mathbf{k}_1 \mathbf{h}_{1,B}] \begin{bmatrix} \mathbf{0}_{[-\Delta_1]^+} & \mathbf{a}[1 : \ell] & \mathbf{0}_{2T} \\ \mathbf{0}_{[\Delta_1]^+} & \mathbf{b}[1 : \ell] & \mathbf{0}_{2T} \\ \mathbf{a}[\ell+1 : 2\ell] & \mathbf{0}_{2T} & \mathbf{a}[2\ell+1 : 3\ell] & \mathbf{0}_{2T} & \mathbf{a}[3\ell+1 : 4\ell] & \mathbf{0}_{[\Delta_1]^+} \\ \mathbf{b}[\ell+1 : 2\ell] & \mathbf{0}_{2T} & \mathbf{b}[2\ell+1 : 3\ell] & \mathbf{0}_{2T} & \mathbf{b}[3\ell+1 : 4\ell] & \mathbf{0}_{[-\Delta_1]^+} \end{bmatrix}.$$

$$\hat{\mathbf{y}}_{R_1,2} = \alpha_1 [-\mathbf{y}_{R_1,2}^*, \mathbf{0}_{2T-|\Delta_1|}, \mathbf{y}_{R_1,1}^*, \mathbf{0}_{2T-|\Delta_1|}, \mathbf{y}_{R_1,4}^*, \mathbf{0}_{2T-|\Delta_1|}, -\mathbf{y}_{R_1,3}^*]$$

$$= \hat{\mathbf{n}}_{R_1,2} + \alpha_1 \sqrt{P_T} [\mathbf{k}_1^* \mathbf{h}_{1,A}^*, \mathbf{k}_1^* \mathbf{h}_{1,B}^*] \begin{bmatrix} \mathbf{0}_{[-\Delta_1]^+} & -\mathbf{a}^*[\ell+1 : 2\ell] & \mathbf{0}_{2T} \\ \mathbf{0}_{[\Delta_1]^+} & -\mathbf{b}^*[\ell+1 : 2\ell] & \mathbf{0}_{2T} \\ \mathbf{a}^*[1 : \ell] & \mathbf{0}_{2T} & \mathbf{a}^*[3\ell+1 : 4\ell] & \mathbf{0}_{2T} & -\mathbf{a}^*[2\ell+1 : 3\ell] & \mathbf{0}_{[\Delta_1]^+} \\ \mathbf{b}^*[1 : \ell] & \mathbf{0}_{2T} & \mathbf{b}^*[3\ell+1 : 4\ell] & \mathbf{0}_{2T} & -\mathbf{b}^*[2\ell+1 : 3\ell] & \mathbf{0}_{[-\Delta_1]^+} \end{bmatrix}.$$

$$\mathbf{y}_A = \hat{\mathbf{n}}_A + \sqrt{P_T} [\alpha_1 \hat{\mathbf{h}}_{1,A,1} \mathbf{k}_1 \mathbf{h}_{1,B}, \alpha_1 \hat{\mathbf{h}}_{1,A,2} \mathbf{k}_1^* \mathbf{h}_{1,B}^*, \alpha_2 \hat{\mathbf{h}}_{2,A,1} \mathbf{k}_2 \mathbf{h}_{2,B}, \alpha_2 \hat{\mathbf{h}}_{2,A,2} \mathbf{k}_2^* \mathbf{h}_{2,B}^*] \mathbf{x}_b \quad (2)$$

$$\underbrace{\begin{bmatrix} \mathbf{0}_{\max\{\tau_{1,B}, \tau_{1,A}\}} & \mathbf{b}[1 : \ell] & \mathbf{0}_{2T} & \mathbf{b}[\ell+1 : 2\ell] & \mathbf{0}_{2T} & \mathbf{b}[2\ell+1 : 3\ell] & \mathbf{0}_{2T} & \mathbf{b}[3\ell+1 : 4\ell] & \mathbf{0}_{[\Delta_A]^+} \\ \mathbf{0}_{\max\{\tau_{1,B}, \tau_{1,A}\}} & -\mathbf{b}^*[\ell+1 : 2\ell] & \mathbf{0}_{2T} & \mathbf{b}^*[1 : \ell] & \mathbf{0}_{2T} & \mathbf{b}^*[3\ell+1 : 4\ell] & \mathbf{0}_{2T} & -\mathbf{b}^*[2\ell+1 : 3\ell] & \mathbf{0}_{[\Delta_A]^+} \\ \mathbf{0}_{\max\{2\tau_{2,A}-\tau_{2,B}, \tau_{2,A}\}} & -\mathbf{b}^*[3\ell : 2\ell+1] & \mathbf{0}_{2T} & -\mathbf{b}^*[4\ell : 3\ell+1] & \mathbf{0}_{2T} & \mathbf{b}^*[\ell : 1] & \mathbf{0}_{2T} & \mathbf{b}^*[2\ell : \ell+1] & \mathbf{0}_{[-\Delta_A]^+} \\ \mathbf{0}_{\max\{2\tau_{2,A}-\tau_{2,B}, \tau_{2,A}\}} & -\mathbf{b}[4\ell : 3\ell+1] & \mathbf{0}_{2T} & \mathbf{b}[3\ell : 2\ell+1] & \mathbf{0}_{2T} & -\mathbf{b}[2\ell : \ell+1] & \mathbf{0}_{2T} & \mathbf{b}[\ell : 1] & \mathbf{0}_{[-\Delta_A]^+} \end{bmatrix}}_{\mathbf{x}_b}$$

$\hat{\mathbf{y}}_{R_{1,1}}$ and $\hat{\mathbf{y}}_{R_{1,2}}$ follow the first and second rows of (1), respectively.

R_2 constructs $\hat{\mathbf{y}}_{R_{2,1}}$ and $\hat{\mathbf{y}}_{R_{2,2}}$ by inserting all-zero row vectors, each with $2T - |\Delta_2|$ elements, between the reverse order of $\mathbf{y}_{R_{2,j}}$ as follows:

$$\begin{aligned} \hat{\mathbf{y}}_{R_{2,1}} &= \alpha_2 [-\hat{\mathbf{y}}_{R_{2,3}}, \mathbf{0}_{2T-|\Delta_2|}, -\hat{\mathbf{y}}_{R_{2,4}}, \mathbf{0}_{2T-|\Delta_2|}, \hat{\mathbf{y}}_{R_{2,1}}, \mathbf{0}_{2T-|\Delta_2|}, \hat{\mathbf{y}}_{R_{2,2}}] \\ &= \hat{\mathbf{n}}_{R_{2,1}} + \alpha_2 \sqrt{P_T} [\mathbf{k}_2^* \mathbf{h}_{2,A}^*, \mathbf{k}_2^* \mathbf{h}_{2,B}^*] \begin{bmatrix} \mathbf{0}_{[\Delta_2]^+} & -\mathbf{a}^*[3\ell : 2\ell+1] & \mathbf{0}_{2T} \\ \mathbf{0}_{[-\Delta_2]^+} & -\mathbf{b}^*[3\ell : 2\ell+1] & \mathbf{0}_{2T} \end{bmatrix} \\ &\quad \begin{bmatrix} -\mathbf{a}^*[4\ell : 3\ell+1] & \mathbf{0}_{2T} & \mathbf{a}^*[\ell : 1] & \mathbf{0}_{2T} & \mathbf{a}^*[2\ell : \ell+1] & \mathbf{0}_{[-\Delta_2]^+} \\ -\mathbf{b}^*[4\ell : 3\ell+1] & \mathbf{0}_{2T} & \mathbf{b}^*[\ell : 1] & \mathbf{0}_{2T} & \mathbf{b}^*[2\ell : \ell+1] & \mathbf{0}_{[\Delta_2]^+} \end{bmatrix}, \\ \hat{\mathbf{y}}_{R_{2,2}} &= \alpha_2 [-\hat{\mathbf{y}}_{R_{2,4}}, \mathbf{0}_{2T-|\Delta_2|}, \hat{\mathbf{y}}_{R_{2,3}}, \mathbf{0}_{2T-|\Delta_2|}, -\hat{\mathbf{y}}_{R_{2,2}}, \mathbf{0}_{2T-|\Delta_2|}, \hat{\mathbf{y}}_{R_{2,1}}] \\ &= \hat{\mathbf{n}}_{R_{2,2}} + \alpha_2 \sqrt{P_T} [\mathbf{k}_2 \mathbf{h}_{2,A}, \mathbf{k}_2 \mathbf{h}_{2,B}] \begin{bmatrix} \mathbf{0}_{[\Delta_2]^+} & -\mathbf{a}[4\ell : 3\ell+1] & \mathbf{0}_{2T} \\ \mathbf{0}_{[-\Delta_2]^+} & -\mathbf{b}[4\ell : 3\ell+1] & \mathbf{0}_{2T} \end{bmatrix} \\ &\quad \begin{bmatrix} \mathbf{a}[3\ell : 2\ell+1] & \mathbf{0}_{2T} & -\mathbf{a}[2\ell : \ell+1] & \mathbf{0}_{2T} & \mathbf{a}[\ell : 1] & \mathbf{0}_{[-\Delta_2]^+} \\ \mathbf{b}[3\ell : 2\ell+1] & \mathbf{0}_{2T} & -\mathbf{b}[2\ell : \ell+1] & \mathbf{0}_{2T} & \mathbf{b}[\ell : 1] & \mathbf{0}_{[\Delta_2]^+} \end{bmatrix}. \end{aligned}$$

where $\hat{\mathbf{y}}_{R_{i,j}} = [\mathbf{y}_{R_{i,j}}[\ell+|\Delta_2|], \mathbf{y}_{R_{i,j}}[\ell+|\Delta_2|-1], \dots, \mathbf{y}_{R_{i,j}}[1]]$, $i = 1, 2$ and $j = 1, 2, 3, 4$.

$\hat{\mathbf{y}}_{R_{2,1}}$ and $\hat{\mathbf{y}}_{R_{2,2}}$ follow the third and fourth rows of (1), respectively.

• In Phase II, R_1 transmits $\hat{\mathbf{y}}_{R_{1,1}}$ from its first antenna and $\hat{\mathbf{y}}_{R_{1,2}}$ from its second antenna; R_2 transmits $\hat{\mathbf{y}}_{R_{2,1}}$ from its first antenna and $\hat{\mathbf{y}}_{R_{2,2}}$ from its second antenna.

At terminal A , after canceling the self-interference on \mathbf{a} , the received signal vector is (2), where $\Delta_A \triangleq \max\{2\tau_{2,A}-\tau_{2,B}, \tau_{2,A}\} - \max\{\tau_{1,B}, \tau_{1,A}\}$.

Example 1: When $\ell = 4$, $[\tau_{1,A}, \tau_{1,B}, \tau_{2,A}, \tau_{2,B}] = [1, 1, 1, 0]$ and $T = 1$. For simplicity, we let $P_T = 1$ and $\alpha_1 = \alpha_2 = 1$.

According to (2), \mathbf{y}_A is

$$\mathbf{y}_A = \hat{\mathbf{n}}_A + [\hat{\mathbf{h}}_{1,A,1} \mathbf{k}_1 \mathbf{h}_{1,B}, \hat{\mathbf{h}}_{1,A,2} \mathbf{k}_1^* \mathbf{h}_{1,B}^*, \hat{\mathbf{h}}_{2,A,1} \mathbf{k}_2 \mathbf{h}_{2,B}, \hat{\mathbf{h}}_{2,A,2} \mathbf{k}_2^* \mathbf{h}_{2,B}^*] \mathbf{x}_b \quad (3)$$

$$\begin{bmatrix} 0 & b[1] & b[2] & 0 & 0 & b[3] & b[4] & 0 & 0 \\ 0 & -b^*[3] & -b^*[4] & 0 & 0 & b^*[1] & b^*[2] & 0 & 0 \\ 0 & 0 & -b^*[6] & -b^*[5] & 0 & 0 & -b^*[8] & -b^*[7] & 0 \\ 0 & 0 & -b[8] & -b[7] & 0 & 0 & b[6] & b[5] & 0 \\ b[5] & b[6] & 0 & 0 & b[7] & b[8] & 0 & 0 & 0 \\ b^*[7] & b^*[8] & 0 & 0 & -b^*[5] & -b^*[6] & 0 & 0 & 0 \\ 0 & b^*[2] & b^*[1] & 0 & 0 & b^*[4] & b^*[3] & 0 & 0 \\ 0 & -b[4] & -b[3] & 0 & 0 & b[2] & b[1] & 0 & 0 \end{bmatrix}.$$

The matrix in (3) can be decomposed into QOSTBC and Alamouti code matrices as

$$\begin{bmatrix} b[2] & b[4] & b[6] & b[8] \\ -b^*[4] & b^*[2] & b^*[8] & -b^*[6] \\ -b^*[6] & -b^*[8] & b^*[2] & b^*[4] \\ -b[8] & b[6] & -b[4] & b[2] \end{bmatrix}, \begin{bmatrix} b[1] & b[3] & 0 & 0 \\ -b^*[3] & b^*[1] & 0 & 0 \\ 0 & 0 & b^*[1] & b^*[3] \\ 0 & 0 & -b[3] & b[1] \end{bmatrix}, \begin{bmatrix} 0 & 0 & b[5] & b[7] \\ 0 & 0 & b^*[7] & -b^*[5] \\ -b^*[5] & -b^*[7] & 0 & 0 \\ -b[7] & b[5] & 0 & 0 \end{bmatrix}$$

where $(b[2], b[4], b[6], b[8])$ form a QOSTBC matrix with stretched signal constellation and $(b[1], b[3]), (b[5], b[7])$ form two Alamouti code matrices. It was proved in that the QOSTBC [31] has single

Table 1: Comparison of ZP-TR QOSTBC, ZP-IR AC [30], and Alamouti code [9] for a network with two single-antenna relays. L is the code length.

Type	Code Rate	Diversity	Complexity
ZP-TR QOSTBC	1 symbol/channel	4	$\mathcal{O}(L S)$
ZP-IR AC	1 symbol/channel	2	$\mathcal{O}(L S ^4)$
Alamouti code	1 symbol/channel	2	$\mathcal{O}(L S)$

symbol decoding complexity. By such decomposed procedure, the ML decoding procedure is significantly facilitated.

3.2. Full Diversity Proof

Theorem 1. *In an asynchronous two-way relay network with two double-antenna relays and maximum delay difference T , ZP-TR QOSTBC achieves full diversity, that is, diversity order 4. The code length is 4ℓ , where $\ell \in \mathbb{Z}_+$.*

Proof: See Appendix. \square

A key insight of designing (1) is that the elements in each row are either all taking their conjugate forms or not taking at all. By doing so, the signal combining vector \mathbf{k}_i can be regarded as part of channel gain as in (2), facilitating the full diversity proof.

3.3. Code Rate Analysis

The worst-case code rate R of ZP-TR QOSTBC is

$$R = \frac{8\ell}{8\ell + 12T + 2 \min\{\tau_{1,A}, \tau_{1,B}, \tau_{2,A}, \tau_{2,B}\}},$$

where 8ℓ is the number of symbols exchanged in both directions. It takes at most $(4\ell + 4T + \min\{\tau_{1,A}, \tau_{1,B}, \tau_{2,A}, \tau_{2,B}\})$ symbol duration to transmit in Phase I, and at most $(4\ell + 8T + \min\{\tau_{1,A}, \tau_{1,B}, \tau_{2,A}, \tau_{2,B}\})$ symbol duration to transmit in Phase II. When ℓ is sufficiently large, R approaches 1 symbol/channel.

3.4. Low-Complexity ML Decoding

Just like Example 1, the codeword \mathbf{X}_b in (2) consists of two parts, namely, $\mathbf{X}_{b,1}$ with QOSTBC structure and $\mathbf{X}_{b,2}$ with Alamouti code structure. For simplicity, the general forms of \mathbf{X}_b is provided in (4) in Appendix. Due to space limit, $\mathbf{X}_{b,1}$ is marked with blue of \mathbf{X}_b in (4), and $\mathbf{X}_{b,2}$ is the remaining columns of \mathbf{X}_b in (4). For $\mathbf{X}_{b,1}$ using stretched constellations, $\mathbf{X}_{b,1}$ follows QOSTBC structure, which is proven in [31] to have single symbol decoding complexity. For $\mathbf{X}_{b,2}$, we jointly decode two Alamouti codes. Therefore, the overall decoding complexity of ZP-TR QOSTBC is $\mathcal{O}(4\ell|S|)$, where $|S|$, the cardinality of the constellation, represents the single symbol decoding complexity, and 4ℓ is the code length.

$$\mathbf{X}_b(\mathbf{b}) = \begin{bmatrix} 0 & \dots & 0 & b[1] & \dots & b[\Delta_A] & b[\Delta_A+1] & \dots & b[\ell] & 0 & \dots & 0 \\ 0 & \dots & 0 & -b^*[1] & \dots & -b^*[\ell+1] & -b^*[\ell+\Delta_A+1] & \dots & -b^*[2\ell] & 0 & \dots & 0 \\ 0 & \dots & 0 & 0 & \dots & 0 & -b^*[3\ell] & \dots & -b^*[2\ell+\Delta_A+1] & -b^*[2\ell+\Delta_A] & \dots & -b^*[2\ell+1] \\ 0 & \dots & 0 & 0 & \dots & 0 & -b[4\ell] & \dots & -b[3\ell+\Delta_A+1] & -b[3\ell+\Delta_A] & \dots & -b[3\ell+1] \\ \hline 0 & \dots & 0 & b[\ell+1] & \dots & b[\ell+\Delta_A] & b[\ell+\Delta_A+1] & \dots & b[2\ell] & 0 & \dots & 0 \\ 0 & \dots & 0 & b^*[1] & \dots & b^*[\Delta_A] & b^*[\Delta_A+1] & \dots & b^*[\ell] & 0 & \dots & 0 \\ 0 & \dots & 0 & 0 & \dots & 0 & -b^*[4\ell] & \dots & -b^*[3\ell+\Delta_A+1] & -b^*[3\ell+\Delta_A] & \dots & -b^*[3\ell+1] \\ 0 & \dots & 0 & 0 & \dots & 0 & b[3\ell] & \dots & b[2\ell+\Delta_A+1] & b[2\ell+\Delta_A] & \dots & b[2\ell+1] \\ \hline 0 & \dots & 0 & b[2\ell+1] & \dots & b[2\ell+\Delta_A] & b[2\ell+\Delta_A+1] & \dots & b[3\ell] & 0 & \dots & 0 \\ 0 & \dots & 0 & b^*[3\ell+1] & \dots & b^*[3\ell+\Delta_A] & b^*[3\ell+\Delta_A+1] & \dots & b^*[4\ell] & 0 & \dots & 0 \\ 0 & \dots & 0 & 0 & \dots & 0 & b^*[\ell] & \dots & b^*[\Delta_A+1] & b^*[\Delta_A] & \dots & b^*[1] \\ 0 & \dots & 0 & 0 & \dots & 0 & -b[2\ell] & \dots & -b[\ell+\Delta_A+1] & -b[\ell+\Delta_A] & \dots & b[\ell+1] \\ \hline 0 & \dots & 0 & b[3\ell+1] & \dots & b[3\ell+\Delta_A] & b[3\ell+\Delta_A+1] & \dots & b[4\ell] & 0 & \dots & 0 \\ 0 & \dots & 0 & -b^*[2\ell+1] & \dots & -b^*[2\ell+\Delta_A] & -b^*[2\ell+\Delta_A+1] & \dots & -b^*[3\ell] & 0 & \dots & 0 \\ 0 & \dots & 0 & 0 & \dots & 0 & b^*[2\ell] & \dots & b^*[\ell+\Delta_A+1] & b^*[\ell+\Delta_A] & \dots & b^*[\ell+1] \\ 0 & \dots & 0 & 0 & \dots & 0 & b[\ell] & \dots & b[\Delta_A+1] & b[\Delta_A] & \dots & b[1] \end{bmatrix} \quad (4)$$

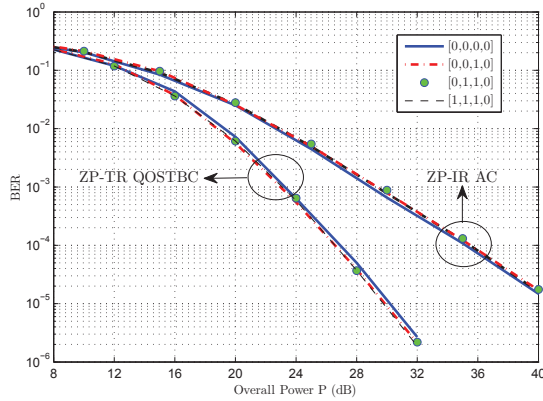


Fig. 2: Comparison among the bit error rate of ZP-TR QOSTBC and ZP-IR AC with 2 bits/symbol and code length $4\ell = 16$.

3.5. Comparisons with Other Codes

Table.1 shows a comparison of ZP-TR QOSTBC, ZP-IR AC [30] and Alamouti code [9]. The code rate of ZP-TR QOSTBC and ZP-IR AC in Table.1 is asymptotic code rate when L is sufficiently large. In ZP-IR AC, interleave reversal procedure causes inter-symbol interference, which adds up the decoding complexity order. In ZP-TR QOSTBC, time reversal, a different construction procedure, avoids such inter-symbol interference and leads to low-complexity ML decoding.

4. SIMULATION RESULTS

The simulation results on the performance of the proposed codes with ML decoding are presented in this section. The channel fading coefficients follow an i.i.d. complex Gaussian distribution with zero mean and unit variance. The maximum delay difference $T = 1$.

Fig. 2 shows the bit error rate (BER) performance of ZP-TR QOSTBC using two double-antenna relays and ZP-IR AC [30] using two single-antenna relays with respect to the total transmit power P , where the transmit power at each terminal and relay is $P/4$, that

is, $P_T = P/4$. The performance of ZP-TR QOSTBC in delay profile $[0, 0, 0, 0]$ can be regarded as that of QOSTBC in the synchronous case. And the performance of ZP-IR AC in delay profile $[0, 0, 0, 0]$ is regarded as that of Alamouti code [9]. The slope difference among these two sets of lines shows the advantage of diversity order 4 over diversity order 2. To achieve BER 10^{-5} , ZP-TR QOSTBC requires overall power around 30 dB, whereas ZP-IR AC requires overall power around 40 dB. Such phenomenon means that considerable power can be saved by using double-antenna relays to achieve the same BER. In asynchronous cases, the code structure of ZP-TR QOSTBC can be decomposed into QOSTBC [31] and Alamouti codes. Such phenomenon is shown in Example 1 by decomposing (3) into a QOSTBC matrix and two Alamouti code matrices. Because of such similarity in code structure between the decomposed code matrices and QOSTBC, the performance of ZP-TR QOSTBC in the asynchronous cases is similar to that of QOSTBC [31] in the synchronous case.

5. CONCLUSION

In this paper, we have proposed a zero-padded time-reversal quasi-orthogonal space-time block code for asynchronous two-way relay networks. The proposed code achieves full diversity order 4 with single symbol ML decoding complexity. Full diversity proof, code rate and decoding complexity analysis were provided for the proposed code design. The simulation verifies the full diversity.

6. APPENDIX - PROOF OF THEOREM 1

Only the case of $\max\{2\tau_{2,A}-\tau_{2,B}, \tau_{2,A}\} > \max\{\tau_{1,B}, \tau_{1,A}\}$ is discussed because of space constraint. Since \mathbf{k}_i does not appear in the codeword matrix, any nonzero vector \mathbf{k}_i will not affect the full diversity gain. Codeword matrix $\mathbf{X}_b(\mathbf{b})$ is shown in (4). $\mathbf{X}_b(\mathbf{b})$ is decomposed into two parts, namely, $\mathbf{X}_{b,1}$ marked in blue of (4) and $\mathbf{X}_{b,2}$, the remaining black columns of (4). $\mathbf{X}_{b,1}$ includes columns with a QOSTBC structure, and $\mathbf{X}_{b,2}$ includes columns with an Alamouti code structure.

Considering that $\mathbf{X}_{b,1}$ has a QOSTBC structure, $\mathbf{X}_{b,1}$ maintains full rank by stretched constellations, which is proven in [31] for QOSTBC. For $\mathbf{X}_{b,2}$, the Alamouti code structure appears on the first two rows and last two rows. Hence, $\mathbf{X}_{b,2}$ guarantees full rank. Therefore, $\mathbf{X}_b(\mathbf{b})$ is full rank in codeword difference matrix, and ZP-TR QOSTBC achieves full diversity.

7. REFERENCES

- [1] T. Cui, F. Gao, T. Ho, and A. Nallanathan, "Distributed space-time coding for two-way wireless relay networks," *IEEE Trans. Signal Process.*, vol. 57, pp. 658–671, Feb. 2009.
- [2] W. Wang, S. Jin, X. Gao, K.-K. Wong, and M.R. McKay, "Power allocation strategies for distributed space-time codes in two-way relay networks," *IEEE Trans. Signal Process.*, vol. 58, pp. 5331–5339, Oct. 2010.
- [3] S. J. Alabed, J. M. Paredes, and A. B. Gershman, "A simple distributed space-time coded strategy for two-way relay channels," *IEEE Trans. Wireless Commun.*, vol. 11, pp. 1260–1265, Feb. 2012.
- [4] Q. Huo, L. Song, Y. Li, and B. Jiao, "A distributed differential space-time coding scheme with analog network coding in two-way relay networks," *IEEE Trans. Signal Process.*, vol. 60, pp. 4998–5004, Sept. 2012.
- [5] S. Zhang, S.-C. Liew, and P. P. Lam, "Physical-layer network coding," in *Proc. ACM Mobicom*, Sept. 24–29, 2006, pp. 358–365.
- [6] S. Zhang, S.-C. Liew, and P. P. Lam, "On the synchronization of physical-layer network coding," in *IEEE Info. Theory Workshop*, Punta del Este, March 13–17, 2006, pp. 404–408.
- [7] L. Lu and S.-C. Liew, "Asynchronous physical-layer network coding," *IEEE Trans. Wireless Commun.*, vol. 11, pp. 819–831, Feb. 2012.
- [8] S. Katti, S. Gollakota, and D. Katabi, "Embracing wireless interference: Analog network coding," in *Proc. Applications, Technology, Architecture, and Protocols for Computer Commun.*, Kyoto, Aug. 27–31, 2007, pp. 397–408.
- [9] S. M. Alamouti, "A simple transmit diversity technique for wireless communications," *IEEE J. Sel. Areas in Commun.*, vol. 16, pp. 1451–1458, Oct. 1998.
- [10] V. Tarokh, H. Jafarkhani, and A. R. Calderbank, "Space-time block coding for wireless communications: performance results," *IEEE J. Sel. Areas in Commun.*, vol. 17, pp. 451–460, Mar. 1999.
- [11] R. W. Heath Jr. and A. J. Paulraj, "Linear dispersion codes for MIMO systems based on frame theory," *IEEE Trans. Signal Process.*, vol. 50, pp. 2429–2441, Oct. 2002.
- [12] B. Hassibi and B. M. Hochwald, "High-rate codes that are linear in space and time," *IEEE Trans. Inf. Theory*, vol. 48, pp. 1804–1824, July 2002.
- [13] X. Li, "Space-time coded multi-transmission among distributed transmitters without perfect synchronization," *IEEE Signal Process. Lett.*, vol. 11, pp. 948–951, Dec. 2004.
- [14] Y. Mei, Y. Hua, A. Swami, and B. Daneshrad, "Combating synchronization errors in cooperative relays," in *Proc. IEEE Int. Conf. Acoustics, Speech, and Signal Processing*, Philadelphia, Mar. 18–23, 2005, vol. 3, pp. 369–372.
- [15] Z. Li and X.-G. Xia, "A simple Alamouti space-time transmission scheme for asynchronous cooperative systems," *IEEE Signal Process. Lett.*, vol. 14, pp. 804–807, Nov. 2007.
- [16] Y. Li, W. Zhang, and X.-G. Xia, "Distributive high-rate space-frequency codes achieving full cooperative and multipath diversities for asynchronous cooperative communications," *IEEE Trans. Veh. Technol.*, vol. 58, pp. 207–217, Jan. 2009.
- [17] S. Wei, D. L. Goeckel, and M. C. Valenti, "Asynchronous cooperative diversity," *IEEE Trans. Wireless Commun.*, vol. 5, pp. 1547–1557, June 2006.
- [18] Y. Shang and X.-G. Xia, "Shift-full-rank matrices and applications in space-time trellis codes for relay networks with asynchronous cooperative diversity," *IEEE Trans. Inf. Theory*, vol. 52, pp. 3153–3167, July 2006.
- [19] M. O. Damen and A. R. Hammons, "Delay-tolerant distributed-TAST codes for cooperative diversity," *IEEE Trans. Inf. Theory*, vol. 53, pp. 3755–3773, Oct. 2007.
- [20] X. Guo and X.-G. Xia, "Distributed linear convolutional space-time codes for asynchronous cooperative communication networks," *IEEE Trans. Wireless Commun.*, vol. 7, pp. 1857–1861, May 2008.
- [21] Z. Zhong, S. Zhu, and A. Nallanathan, "Delay-tolerant distributed linear convolutional space-time code with minimum memory length under frequency-selective channels," *IEEE Trans. Wireless Commun.*, vol. 8, pp. 3944–3949, Aug. 2009.
- [22] N. Wu and H. Gharavi, "Asynchronous cooperative MIMO systems using a linear dispersion structure," *IEEE Trans. Veh. Technol.*, vol. 59, pp. 779–787, Feb. 2010.
- [23] M. R. Bhatnagar, A. Hjørungnes, and M. Debbah, "Delay-tolerant decode-and-forward based cooperative communication over Ricean channels," *IEEE Trans. Wireless Commun.*, vol. 9, pp. 1277–1282, Apr. 2010.
- [24] M. Sarkiss, G. R. B. Othman, M. O. Damen, and J. C. Belfiore, "Construction of new delay-tolerant space-time codes," *IEEE Trans. Inf. Theory*, vol. 57, pp. 3567–3581, June 2011.
- [25] W. Wang, F.-C. Zheng, A. Burr, and M. Fitch, "Design of delay-tolerant linear dispersion codes," *IEEE Trans. Commun.*, vol. 60, pp. 2560–2570, Sept. 2012.
- [26] Y. Liu, W. Zhang, S. C. Liew, and P. C. Ching, "Bounded delay-tolerant space-time codes for distributed antenna systems," *IEEE Trans. Wireless Commun.*, vol. 13, pp. 4644–4655, Aug. 2014.
- [27] H.-M. Wang, X.-G. Xia, and Q. Yin, "A linear analog network coding for asynchronous two-way relay networks," *IEEE Trans. Wireless Commun.*, vol. 9, pp. 3630–3637, Dec. 2010.
- [28] Z. Li, X.-G. Xia, and B. Li, "Achieving full diversity and fast ML decoding via simple analog network coding for asynchronous two-way relay networks," *IEEE Trans. Commun.*, vol. 57, no. 12, pp. 3672–3681, Dec. 2009.
- [29] Z. Fang, F. Liang, S. Zhang, and T. Peng, "A cyclic shift relaying scheme for asynchronous two-way relay networks," *Wireless Personal Commun.*, vol. 71, pp. 2863–2876, Aug. 2013.
- [30] Y. Liu, W. Zhang, S. C. Liew, and P. C. Ching, "Achieving full-diversity and fast maximum likelihood decoding in asynchronous analog network coding," in *Proc. IEEE Int. Conf. Acoustics, Speech, and Signal Processing*, Florence, May 4–9, 2014, pp. 4312–4316.
- [31] P. Marsch, W. Rave, and G. Fettweis, "Quasi-orthogonal STBC using stretched constellations for low detection complexity," in *Proc. IEEE Wireless Commun. and Networking Conf.*, Kowloon, March 11–15, 2007, pp. 757–761.